# SECOND-ORDER CHANNEL PARAMETER ESTIMATION ASSISTED CANCELLATION OF CHANNEL VARIATION-INDUCED INTER-SUBCARRIER INTERFERENCE IN OFDM SYSTEMS

Matthias Münster and Lajos Hanzo[1]

Dept. of ECS, Univ. of Southampton, SO17 1BJ, UK.
Tel: +44-1703-593 125, Fax: +44-1703-594 508
Email:lh@ecs.soton.ac.uk, http://www-mobile.ecs.soton.ac.uk

## ABSTRACT

**OFDM transmission is known to be sensitive against carrier frequency offsets, as well as against the channel impulse response (CIR) variations incurred during an OFDM symbol period. Both of these phenomena lead to inter-subcarrier interference (ICI). Here we will concentrate on the latter phenomenon. ICI can be considered as an additional noise contribution, which linearly depends on the signal power and thus it potentially limits the achievable BER at relatively high SNRs. In this contribution we propose a second-order time-domain CIR tap variation estimator, which relies on both the received signal as well as on tentative symbol decisions. Our simulation results obtained in the context of a system employing decision-directed channel-prediction demonstrate that with the aid of the proposed algorithm, ICI cancellation can be performed even in high Doppler frequency channel scenarios. This is achieved without inserting additional time-domain pilot symbols.**

## 1. INTRODUCTION

OFDM transmission is known to be sensitive against the variations of the channel impulse response (CIR) taps during the OFDM symbol period. Specifically, a loss of orthogonality between the subcarrier transfer functions is observed, which results in inter-subcarrier interference (ICI). In each subcarrier the ICI contribution can be viewed as additional noise which is - assuming a sufficiently high number of subcarriers - near-Gaussian distributed. However, in contrast to the AWGN, the ICI in different subcarriers is correlated. Since the ICI power is a linear function of the signal power, the AWGN power may be exceeded by the ICI power for sufficiently high signal levels. Several schemes have been proposed in the literature for reducing the ICI noise power [1–3]. For example, Hasholzner *et al.* [1] propose to model the ICI generation by means of a Multiple-Input Multiple-Output (MIMO) system. Equalized and potentially less ICI contaminated subcarrier signals are obtained by a weighted superposition of the signal received in each subcarrier with the contributions from its neighbours. Adaptation of the frequency domain MIMO equalizer weights is achieved by means of the Recursive Least Squares (RLS) algorithm upon invoking the difference between the complex signals at the symbol detector output and at the equalizer output. A drawback of this approach is the RLS algorithm's limited CIR tracking capability under rapid fading channel conditions. An algorithm which follows a similar strategy was proposed in [2]. Here the equalizer weights are obtained by directly inverting the channel matrix describing the MIMO system inflicting the ICI. This approach is equivalent to de-coupling the subcarriers. However, the dimension of the channel matrix is in most cases excessive for direct inversion. Hence, the inversion of multiple lower-dimensional sub-matrices hosting only a limited subset of complex ICI transfer factors between the subcarrier to be decontaminated and its nearest neighbours was proposed in both [1] and [2]. Since the rate of change of the CIR tap values is limited by the channel's Doppler frequency, the ICI is is predominantly restricted to neighbouring subcarriers. The estimation of the channel matrix was achieved in [2] upon regularly inserting time-domain pilot symbols into the OFDM symbol stream. More specifically, the channel sounding symbol was a Dirac-impulse like time-domain pilot tone surrounded by zero-samples, where the length of each zero-segment was identical to that of the OFDM symbol's cyclic prefix. For the simulations presented in [2], a propagation scenario having a relatively small delay spread was assumed, since otherwise the additional channel-sounding overhead would have been prohibitive. In the context of the Wireless Asynchronous Transfer Mode (WATM) system model, 512 subcarriers and a 64-sample guard interval were assumed [4]. Using the channel sounding symbols proposed in [2], this would impose a pilot overhead of 25%, which is excessive. A potential solution requiring no additional pilot information for estimating the CIR tap's variation will be detailed in Sections 3 of our contribution. Another approach which we would like to mention is that of Hutter *et al.* [3], where a reduction of the ICI was achieved upon exploiting the correlation between the ICI contributions im-

EUROCON '2001, 5-7 JULY 2001, BRATISLAVA, SLOVAK REPUBLIK

The financial support of the European Union under the auspices of the Pan-European TRUST project and that of the EPSRC, Swindon UK is gratefully acknowledged

posed on adjacent subcarriers. In contrast to the algorithms outlined in [1, 2], in [3] no explicite knowledge concerning the frequency domain MIMO channel transfer factors between the different subcarriers was invoked. An estimate of the short-term channel correlation matrix was obtained by evaluating the vector of error signals between the sliced and remodulated symbol and the received symbol for each subcarrier, followed by multiplication with its Hermitean transpose. A refinement was achieved through averaging with the corresponding tentative estimate associated with the previous OFDM symbol period. The rest of the paper is organized as follows. In Section 2 the mechanismens of ICI generation will be reviewed, followed by an evaluation of the potentially achievable ICI reduction. The CIR tap variation estimator will be detailed in Section 3, while the ICI canceller is described in Section 4. The system's BER performance is characterized in Section 5 and we will draw our conclusions in Section 6.

## 2. THE SIGNAL MODEL

It has been demonstrated for example in [2] that the signal $x[n,k]$ received in the $k$-th subcarrier of the $n$-th OFDM symbol is a weighted superposition of the complex symbol $s[n,k]$ assigned to this subcarrier at the transmitter, with the contributions $s[n,\acute{k}]$ from all other subcarriers $\acute{k} \neq k$:

$$x[n,k] = \sum_{\acute{k}=0}^{N-1} \left( \sum_{m=0}^{M-1} H_m[n,k-\acute{k}] e^{-j\frac{2\pi}{N}m\acute{k}} \right) s[n,\acute{k}] + \\ + n[n,k], \quad (1)$$

where:

$$H_m[n,k-\acute{k}] = \frac{1}{N} \sum_{t=0}^{N-1} h_m[n,t] e^{-j\frac{2\pi}{N}t(k-\acute{k})}, \quad (2)$$

$$n[n,k] = \sum_{t=0}^{N-1} \acute{n}[n,t] e^{-j\frac{2\pi}{N}tk}. \quad (3)$$

Specifically, $H_m[n,k-\acute{k}]$ defined in Equation 2 denotes the $(k-\acute{k})$-th frequency bin of the DFT associated with the complex time-domain fading signal $h_m[n,t]$ of the $m$-th CIR tap during the $n$-th OFDM symbol period - normalized to the number of subcarriers $N$. Furthermore, $n[n,k]$ is the $k$-th DFT bin of the complex time-domain AWGN noise process $\acute{n}[n,t]$, again for the $n$-th OFDM symbol period. The term $M-1$ represents the maximum multipath-delay imposed by the channel, given as an integer multiple of the sampling interval duration $T_s$. It should be noted that in Equation 1 the contributions for $k \neq \acute{k}$ constitute the ICI inflicted by the neighbouring subcarriers upon the $k$-th subcarrier. In [3, 5] the variance of the ICI has been evaluated, employing the standard definition $\sigma^2_{ICI} = E\{x[n,k]x^*[n,k]|_{k\neq\acute{k}}\}$ with the aid of Equation 1, where $E\{\}$ denotes the expectation. Similarly, we can evaluate the variance of the residual ICI, $\sigma^2_{ICI,resid}$ at the output of an ideal ICI cancellation scheme which is capable of suppressing the undesired ICI contributions in the range of $\{k-sym,\ldots,k+sym\}\backslash\{k\}$ around the subcarrier $k$, as follows:

| *matrix_size* | 1 | 3 | 5 |
|---|---|---|---|
| $\sigma^2_{ICI,cancel}/\sigma^2_s\|_{lin}$ | 0.012896 | 0.005008 | 0.003063 |
| $reduction\|_{dB}$ | | -4.108 | -2.135 |

Table 1: *Residual* ICI variance normalized to the signal variance for an OFDM symbol normalized Doppler frequency of $f_dT_f = 0.1$ in the context of the indoor WATM channel environment using $N = 512$ and $N_g = 64$.

$$\frac{\sigma^2_{ICI,resid}}{\sigma^2_s} = 1 - \frac{1}{N^2}\Bigg[(1+2\cdot sym)N + \\ + 2\sum_{\Delta n=1}^{N-1}(N-\Delta n)\frac{sin\left((sym+\frac{1}{2})\frac{2\pi}{N}\Delta n\right)}{sin\left(\frac{\pi}{N}\Delta n\right)} \cdot \\ \cdot J_0\left(2\pi T_s f_D \Delta n\right)\Bigg], \quad (4)$$

where a normalization to the signal variance $\sigma^2_s$ has been performed. In Equation 4, $J_0()$ denotes the zero-order Bessel function of the first kind, assuming Jakes fading [6], $T_s$ is the sampling interval duration and $f_D$ is the maximum Doppler frequency of the channel. It should be noted that by setting the one-sided ICI cancellation range $sym$ equal to zero, Equation 4 degenerates into the corresponding expression for the ICI noise variance given in [3, 5]. We have evaluated Equation 4 for channel sub-matrix sizes of 1, 2 and 4, where the sub-matrix size is related to the one-sided ICI cancellation range according to $matrix\_size = 1 + 2 \cdot sym$. Hence, a sub-matrix size of 1 corresponds to the case of no ICI cancellation. Here we employed the parameters of the indoor WATM system model [4]. Specifically $N = 512$ and $f_dT_f = 0.1$ was assumed as a worst-case scenario, where $T_f$ denotes the frame duration, which is related to the sampling interval duration $T_s$ by $T_f = (N+N_g)T_s$, with $N_g$ as the number of guard samples. The results are listed in Table 1, where we have also calculated the differential ICI variance reduction in terms of $dB$, achieved by increasing the ICI cancellation range. In accordance with [2] the highest improvement is achieved by employing ICI cancellation with a one-sided range of 1 instead of no cancellation. Specifically this results in an ICI reduction of about $4.1dB$. A prerequisite for attaining this performance is the availability of perfect channel- and error-free symbol knowledge, so that the ICI contributions can be perfectly reconstructed and subtracted from the received signal. Upon invoking Equation 4 and by considering the first two elements of the Taylor approximation of $J_0(x)$, which is $\tilde{J}_0(x) = 1 - \frac{1}{4}x^2 \; \forall \; x \ll 1$ [7], we also confirm that in the range of $f_DT_f$ of interest, the ICI variance is proportional to the square of the Doppler frequency $f_D$: $\sigma^2_{ICI,red} = c \cdot f_D^2\sigma^2_s$, where $c$ is the proportionality constant inherent in Equation 4. We conclude furthermore that the maximum achievable ICI reduction is independent of the Doppler frequency $f_D$. In the next section we will embark on a description of the system model.

## 3. CHANNEL ESTIMATION

In Section 1 we outlined that a prerequisite for the cancellation of CIR variation induced ICI considered here is the availability of an estimate of the variation of each CIR tap during a specific OFDM symbol period. In contrast to [2], our aim is to avoid using dedicated time-domain pilot symbols while also circumventing the employment of an iterative MIMO equalizer weight update strategy. **Explicitely, our strategy is to obtain tentative symbol decisions without using ICI cancellation in a first iteration, followed by an estimation of the CIR tap variations on the basis of these tentative symbol decisions and by also capitalizing on the knowledge of the received time-domain signal. This is followed by frequency-domain ICI cancellation and a final iteration to obtain symbol decisions on the basis of a potentially less ICI-contaminated signal.** Hence, our aim in this section is to develop the CIR tap variation estimator. The received time domain signal $r[n,t]$, $t \in \{0,\ldots,N-1\}$ within the FFT window of the $n$-th OFDM symbol period is given by the convolution of the time-variant CIR tap values $h_m[n,t]$, where $m \in \{0,\ldots,M-1\}$ denotes the tap index, with the output $t[n,t]$ of the OFDM modulator, yielding:

$$r[n,t] = \sum_{m=0}^{M-1} h_m[n,t]t[n,t-m] + \acute{n}[n,t]. \quad (5)$$

Here we follow the philosophy that the evolution of each CIR tap value during the FFT window of an OFDM symbol period can be linearly approximated, which was also advocated in [2], resulting in:

$$\tilde{h}_m[n,t] = \tilde{c}_m[n] \cdot t + \tilde{b}_m[n], \quad (6)$$

where $\tilde{c}_m[n]$ and $\tilde{b}_m[n]$, $m \in \{0,\ldots,M-1\}$ are the CIR tap variation estimator coefficients to be determined. Hence, a cost-function given by the aggregate mean-square error between the received time-domain signal and the appropriately synthesized signal can be defined as follows:

$$C[n] = \sum_{t=0}^{N-1} \left| r[n,t] - \sum_{m=0}^{M-1} (\tilde{c}_m[n]t + \tilde{b}_m[n])t[n,t-m] \right|^2. \quad (7)$$

In order to determine the estimator coefficients $\tilde{c}_m[n]$ and $\tilde{b}_m[n]$ for all $m \in \{0,\ldots,M-1\}$, a suitable approach is to minimize Equation 7 using standard optimization techniques, namely by evaluating the partial derivatives with respect to the desired variables:

$$\frac{\partial C[n]}{\partial \tilde{b}_m[n]} = \sum_{t=0}^{N-1} \left\{ -r^*[n,t]t[n,t-m] + \right. \quad (8)$$
$$\left. + \sum_{\acute{m}=0}^{M-1} (\tilde{c}^*_{\acute{m}}t + \tilde{b}^*_{\acute{m}}) \cdot t[n,t-m]t^*[n,t-\acute{m}] \right\},$$

and

$$\frac{\partial C[n]}{\partial \tilde{c}_m[n]} = \sum_{t=0}^{N-1} \left\{ -r^*[n,t] \cdot t \cdot t[n,t-m] + \right. \quad (9)$$
$$\left. + \sum_{\acute{m}=0}^{M-1} (\tilde{c}^*_{\acute{m}}t + \tilde{b}^*_{\acute{m}}) \cdot t \cdot t[n,t-m]t^*[n,t-\acute{m}] \right\}.$$

At the optimum point the partial derivatives $\partial C[n]/\partial \tilde{b}_m$ and $\partial C[n]/\partial \tilde{c}_m$ are zero for all $m \in \{0,\ldots,M-1\}$. Hence, a system of equations can be established assuming knowledge of the received signal $r[n,t]$ and that of the transmitted signal $t[n,t]$, yielding estimates for the desired estimator coefficients upon inverting a matrix of dimensions $2M \times 2M$. In [8] it was proposed - assuming a similar estimation problem - to identify the path delays exhibiting the highest signal power and hence only to incorporate these so-called significant taps in the estimation process. This could be achieved with the aid of dedicated OFDM training symbols employed in the context of decision-directed channel estimation [6, 9]. The advantage would potentially be a significant size reduction of the matrix to be inverted. In the next section we will outline a range of different ICI cancellation schemes applicable to our system.

## 4. CANCELLATION SCHEMES

We commence with a brief review of the most prominent ICI-cancellation schemes employed. Let us recall Equation 1, which established a relationship between the symbols $s[n,\acute{k}]$ transmitted in different subcarriers $\acute{k}$ and the complex symbol $x[n,k]$ received on the $k$-th subcarrier, as a function of the subcarrier coupling factors and that of the channel noise. This relation could also be expressed in matrix form, potentially leading to an $N \times N$ frequency domain MIMO channel matrix, where $N$ denotes the number of subcarriers. Fully compensating for the effects of ICI would require as alluded to in Section 2 the inversion of the channel matrix, which is impractical in terms of computational complexity. Hence, a more practical solution is to exploit the band structure of the channel matrix, which is a direct consequence of the sharply decaying ICI influence as a function of the frequency-domain separation of subcarriers. This is a ramification of the relatively low Doppler frequency in comparison to the OFDM symbol's bandwidth. Therefore we perform ICI cancellation only for a limited subset of the subcarriers, namely within a range of $sym$ around the subcarrier considered [1, 2]. Hence, for the $k$-th subcarrier a simplified relation between the transmitted symbol $s[n,k]$ and the received symbol $x[n,k]$ - assuming a cancellation range of $sym = 1$ is given by [2]:

$$\mathbf{x}[k] = \mathbf{H}[k]\mathbf{s}[k] + \mathbf{n}_r[k], \quad (10)$$

where

$$\mathbf{x}[k] = (x[k-1], x[k], x[k+1])^T \quad (11)$$
$$\mathbf{s}[k] = (s[k-1], s[k], s[k+1])^T \quad (12)$$
$$\mathbf{n}_r[k] = (n_r^k[k-1], n_r^k[k], n_r^k[k+1])^T, \quad (13)$$

and

$$\mathbf{H}[k] = \begin{pmatrix} H[k-1,k-1] & H[k-1,k] & 0 \\ H[k,k-1] & H[k,k] & H[k,k+1] \\ 0 & H[k+1,k] & H[k+1,k+1] \end{pmatrix}. \quad (14)$$

For notational convenience we have omitted the OFDM symbol index $n$. The vector $\mathbf{n}_r[k]$ of residual noise contributions requires further explanation. Each of its elements

$n_r^k[x]$ is constituted by the sum of the AWGN in the $x$-th subcarrier and the residual ICI taking into account the partial ICI cancellation. For example, following from the structure of the matrix $\mathbf{H}[k]$ defined in Equation 14, the residual ICI contribution in the $(k-1)$-th subcarrier is identical to the original contribution minus the contribution from the $k$-th subcarrier. By contrast, the residual ICI in the $k$-th subcarrier is constituted by the difference between the original contribution in this subcarrier minus the interference due to the $(k-1)$-th and the $(k+1)$-th subcarrier. The elements of the matrix $\mathbf{H}[k]$ can be directly inferred from Equation 1, specifically from the term in round brackets. Equation 10 suggests several approaches for recovering the symbol transmitted on the $k$-th subcarrier. The authors of [2] proposed the direct inversion of the partial channel matrix $\mathbf{H}[k]$, which will be referred to during our comparative study as the **zero-forcing (ZF)** solution. Hence, the signal at the output of the combiner is given by:

$$\tilde{\mathbf{s}}_{ZF}[k] = \mathbf{H}^{-1}[k]\mathbf{x}[k], \tag{15}$$

where finally only the desired element in the center of the vector $\tilde{\mathbf{s}}_{ZF}[k]$ is retained. An exception is given by the first and the last vector of recovered symbols, where the first $sym+1$ elements and the last $sym+1$ elements are retained [2], respectively. A well-known disadvantage of the ZF solution is the associated potential noise amplification. A more attractive, but also more complex approach is the **minimum mean-square error (MMSE)** solution, which was also advocated in [3]:

$$\tilde{\mathbf{s}}_{MMSE}[k] = \left(\mathbf{H}^H[k]\mathbf{H}[k] + \left(\frac{\sigma^2_{n,\sum}}{\sigma^2_s} + dl\right)\mathbf{I}\right)^{-1} \mathbf{H}^H[k]\mathbf{x}[k]. \tag{16}$$

It should be noted that in contrast to [3] we have not taken into account the correlation between the residual ICI associated with the subcarriers encompassed by the partial MIMO channel matrix $H[k]$, since the merit of doing so appears to be relatively limited. The residual noise variance $\sigma^2_{n,\sum}$ in Equation 16 is given by the sum of the AWGN noise variance $\sigma^2_n$ and the residual ICI variance $\sigma^2_{ICI,cancel}$, where in the context of our simulations we have employed the estimated noise variance given in the second column of Table 1. Furthermore, in Equation 16, $dl$ denotes a diagonal loading constant, which is often employed in the literature [3] for facilitating the inversion of ill-conditioned matrices. In the context of our simulations in Section 5 we experimentally found a value of $dl = 0.055$ to operate best for BPSK and $dl = 0$ for QPSK. A third approach to ICI cancellation, which - in contrast to the previously mentioned ZF- and MMSE solutions - requires the knowledge of the transmitted symbols, is that of **subtractive cancellation**, which is defined here simply by the subtraction of the reconstructed from the received signal. This can be expressed as:

$$\tilde{\mathbf{s}}_{MMSE}[k] = r[k] - \sum_{\substack{\acute{k}=k-sym \\ \acute{k}\neq k}}^{k+sym} H[k,\acute{k}]\hat{s}[\acute{k}], \tag{17}$$

where $\hat{s}[\acute{k}]$ denotes the tentative symbol decision of the $\acute{k}$-th subcarrier symbol obtained during the first iteration. In next section the above ICI cancellation schemes will be characterized in conjunction with the CIR tap variation estimator introduced in Section 3.

## 5. SIMULATION RESULTS

In this section we will assess the performance of the proposed system using a decision-directed channel estimator similar to that proposed in [6] for obtaining initial symbol decisions. In [6] Wiener filtering of the CIR taps in the time-domain is employed for obtaining a potentially less noise-contaminated estimate of the channel transfer function for the current timeslot, which is then employed as an initial channel estimate during the next timeslot. This implies assuming the invariance of the channel transfer function between two consecutive OFDM symbols. By contrast, we employ a Wiener prediction filter in order to compensate for the CIR tap variations actually incurred in the high-Doppler propagation scenarios considered here. As outlined in [9], the conceptual difference between the interpolation and the prediction filter resides in the structure of the co-variance vector, which is part of the Wiener equation. In our simulations we employed a decision-directed channel estimator capitalizing on an 8-tap CIR predictor, a training period of 32 OFDM symbols and a training block length of two OFDM symbols. It should be noted that the training period or equivalently the time-domain distance between two training blocks is a crucial parameter, especially at low SNRs, where error propagation is known to deteriorate the decision-directed channel estimator's performance. The training block length has two implications. Firstly, at low SNRs error propagation extending over the training period is experienced as the result of using past CIR estimates in the process of CIR tap prediction. Secondly, the CIR tap predictor is required to deliver sufficiently accurate channel estimates already during the reception of the first information-bearing OFDM symbol. It should be noted that the proposed CIR tap variation estimator could also be employed in a system, which invokes for example frequency-domain pilot symbols for obtaining a tentative CIR estimate, in order to assist in the tentative initial demodulation required. Our simulations have been conducted in the context of the 512-subcarrier indoor WATM channel [4] employing a worst-case Doppler scenario of $f_D T_f = 0.1$. Our BER results for BPSK modulation are portrayed in Figure 1, while those for QPSK modulation are depicted in Figure 2. In both figures we have also plotted the system's performance without ICI cancellation. We considered both, a "frame-invariant" fading scenario, where the fading envelope was kept constant during an OFDM symbol period in order to avoid the generation of ICI, and a "frame-variant" fading scenario. We observe that even in the context of "frame-invariant" fading, where no ICI was generated, the BER performance is limited at high SNRs, which is attributed to the imperfections of the CIR predictor. Amongst the different ICI cancellation schemes the MMSE canceller exhibits the best performance. Specifically, in the context of BPSK the BER is reduced by a factor of 5, while in conjunction with QPSK a reduction by a factor of 3 is observed. The BER difference between these

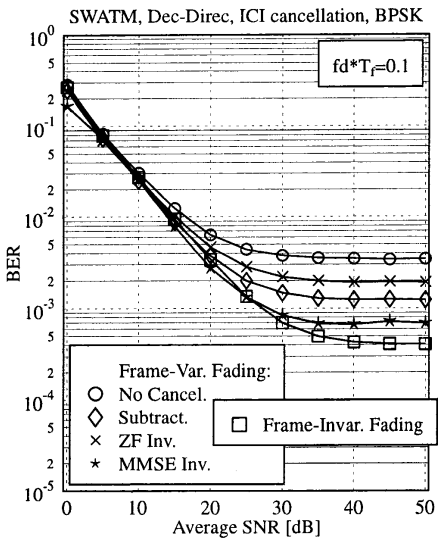


Figure 1: BER performance of a system employing 8-tap Wiener filter prediction assisted decisions-directed channel estimation and two-stage ICI cancellation according to Sections 3 and 4 by using **BPSK modulation**.

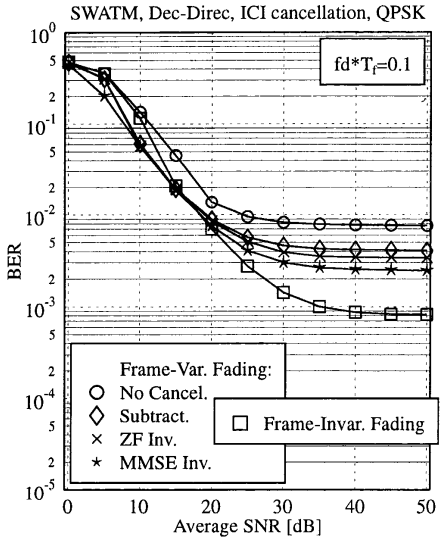


Figure 2: BER performance of a system employing 8-tap Wiener filter prediction assisted decisions-directed channel estimation and two-stage ICI cancellation according to Sections 3 and 4 by using **QPSK modulation**.

schemes can be explained by pointing out that the minimum distance between signal points hosted by a QPSK constellation are located closer to each other than in the BPSK constellation and hence a higher vulnerability against channel estimation errors and channel noise can be observed. Another phenomenon, which requires further explanation is that for BPSK the ZF-inversion performs worse, than subtraction based cancellation. By contrast, for QPSK the situation was reversed. An explanation is that in the case of BPSK, when relatively reliable first-iteration symbol decisions are available, the subtractive combiner does not encounter the problem of noise amplification, which was associated with the ZF-inversion based solution. Again, by contrast, for QPSK more erroneous symbol decisions are employed in the subtractive cancellation process and hence the ZF-inversion, which does not capitalize directly on tentative symbol decisions is advantageous.

## 6. CONCLUSION

In this contribution we have demonstrated the feasibility of CIR tap variation-induced ICI cancellation without requiring additional time-domain pilot symbols as in [2] or without necessitating iterative weight update techniques as in [1]. We employed a two-stage detection technique, where during the first iteration tentative symbol decisions are provided on the basis of the initially ICI-contaminated received signal. These initial estimates are then employed to estimate the CIR tap variations incurred during the current OFDM symbol period. Following the process of ICI cancellation, the potentially less ICI-impaired received signal is employed in a second demodulation iteration to provide symbol decisions. As a result, the BER was reduced by a factor of five in the context of BPSK and a factor of three in the context of QPSK, when using decision-directed channel estimation as a basis for first-stage detection.

## 7. REFERENCES


[1] R. Hasholzner, C. Drewes, and A. Hutter, "Untersuchungen zur linearen ICI-Kompensation bei OFDM (in German)," in *3.OFDM Fachgespräch*, Technische Universität Braunschweig, Germany, Sept. 1998.

[2] W. G. Jeon, K. H. Chang, and Y. S. Cho, "An Equalization Technique for Orthogonal Frequency-Division Multiplexing Systems in Time-Variant Multipath Channels," *IEEE Trans. on. Comms.*, vol. 47, pp. 27–32, Jan 1999.

[3] A. Hutter and R. Hasholzner, "Determination of Intercarrier Interference Covariance Matrices and their Application to Advanced Equalization for Mobile OFDM," in $5^{th}$ *International OFDM-Workshop 2000*, pp. 33/1–33/5, Technische Universität Hamburg-Harburg, Sept. 2000.

[4] L. Hanzo, W. Webb, and T. Keller, *Single- and Multi-carrier Quadrature Amplitude Modulation.* IEEE Press- John Wiley, April 2000.

[5] M. Ruessel and G. L. Stüber, "Terrestrial digital video broadcasting for mobile reception using OFDM," *Wireless Pers. Commun.*, vol. 2, no. 3, pp. 45–66, 1995.

[6] Y. Li, L. J. Cimini, and N. R. Sollenberger, "Robust Channel Estimation for OFDM Systems with Rapid Dispersive Fading Channels," *IEEE Trans. on. Comms.*, vol. 46, pp. 902–915, Apr 1998.

[7] W. H. Press, S. A. Teukolshy, W. T. Vetterling, and B. P. Flannery, *Numerical Recipes in C.* Cambridge University Press, 1992.

[8] Y. Li, N. Seshadri, and S. Ariyavisitakul, "Channel Estimation for OFDM Systems with Transmitter Diversity in Mobile Wireless Channels," *IEEE Journal on Sel. Areas in Comms.*, vol. 17, pp. 461–471, March 1999.

[9] M. Münster and L. Hanzo, "MMSE Channel Prediction For Symbol-by-symbol Adaptive OFDM Systems," in $5^{th}$ *International OFDM-Workshop 2000*, pp. 35/1–35/6, Technische Universität Hamburg-Harburg, Sept. 2000.